

Mice produce ultrasonic vocalizations by intra-laryngeal planar impinging jets

Elena Mahrt¹, Anurag Agarwal², David Perkel³,

5 Christine Portfors¹, Coen P.H. Elemans^{4,*}

Affiliations:

1. Washington State University, Vancouver, WA 98686, USA
2. Department of Engineering, University of Cambridge, Cambridge CB2 1PZ, United Kingdom
3. Departments of Biology and Otolaryngology, University of Washington, Seattle, WA 98195, USA
- 10 4. Department of Biology, University of Southern Denmark, DK-5230 Odense, Denmark

* Email to: coen@biology.sdu.dk

Rodent ultrasonic vocalizations (USVs) are a vital tool for linking gene mutations to behavior in mouse
15 models of communication disorders, such as autism [1]. However, we currently lack an understanding of
how physiological and physical mechanisms combine to generate acoustic features of the vocalizations,
and thus cannot meaningfully relate those features to experimental treatments. Here we test and provide
10 evidence against the two leading hypotheses explaining USV production: superficial vocal fold
vibrations [2], and a hole-tone whistle [3]. Instead we propose and provide theoretical and experimental
20 evidence for an alternative and novel vocal mechanism, a glottal jet impinging onto the laryngeal inner
planar wall. Our data provide a framework for future research on the neuromuscular control of mouse
vocal production and for interpreting mouse vocal behavior phenotypes.

Murine rodents produce USVs with complex acoustic song-like structure that play important
social roles, such as mating and territory defense [4]. USVs are emitted between 30 -100 kHz peak

25 frequency (F_p) and often contain instantaneous F_p jumps separated by 15-35 kHz. USVs are
hypothetically produced by a hole-tone whistle mechanism (Hypothesis 1), where two spaced circular
orifices generate a whistle [3] akin to the teakettle whistle [5]. These sounds are produced without
structural motion, only aerodynamic and acoustic feedback. In rats, the F_p of USVs shifted upwards in
lower density heliox atmosphere, supporting this mechanism [3]. The first orifice would be the glottis,
30 and the location of the second orifice would be either a) the oropharyngeal opening leading to the
mouth, b) the epiglottis in semiclosed position, or c) superior vocal folds. Identification of the
production mechanism and these constrictions is crucial for understanding the (constraints on) neural
control of F_p and other acoustic parameters [6]. Alternatively, USVs could be produced by oscillation of
only superficial vocal fold layers (Hypothesis 2), akin to the human “whistle” falsetto mode [2] where
35 the effective oscillating mass is reduced compared to normal chest voice allowing higher oscillation
frequencies.

To test these hypotheses, we studied sound production in excised mouse larynges using high-
speed imaging (100,000 frs/sec) of the vocal folds. With adducted vocal folds, a glottal opening was
located between the arytenoid cartilages on the dorsal side of the larynx (**Fig 1A,B**). Above subglottal
40 air flow of 1-2 ml/s, USVs were readily elicited in the larynges of 15 animals (7 females and 8 males).
The frequencies of *in vitro* USVs corresponded well to *in vivo* USVs (**Fig S1**). We extracted glottal
shape parameters (N=5) from high-speed video (**Fig 1B**). Glottal width did not oscillate at sound
frequencies (**Fig 1C**), arguing against an oscillating vocal fold origin of USVs (contra Hypothesis 2).
These data suggest that if mice use a hole-tone whistle mechanism to produce USVs, both constrictions
45 must be confined within the larynx.

To test if USVs are produced by a hole-tone whistle mechanism and determine the location of
the second constriction, we subsequently removed the epiglottis and thyroid cartilage to just above the

vocal folds. Removal of the epiglottis silenced the larynx in 2 out of 7 animals, but upper thyroid removal silenced 7 out of 7 preparations (Fig 1D), which suggests the upper thyroid is essential to USV production. To further test this hypothesis, we replaced the upper thyroid with a metal plate (N=5);
50 USVs recovered 100% after rescue. Because USVs are generated without a second constriction present, these observations are inconsistent with the hole-tone mechanism (contra Hypothesis 1).

Self-sustained whistles can occur when an air jet impinges on an object, a phenomenon that has predominantly received attention for supersonic and high-speed subsonic flows [7-9]. The tones are
55 caused by a feedback loop between coherent flow structures travelling downstream and acoustic waves travelling upstream in the flow [7]. Feedback could also happen in reverberating acoustic conditions. Both rat and mouse *in vivo* USVs and our *in vitro* data clearly show stable frequency modes and jumps between modes, indicating this system is resonance driven.

We propose that rodent USVs are produced by feedback between downstream convecting
60 coherent flow structures from the glottis and upstream-propagating acoustic waves. The downstream convecting flow structures are generated by instabilities in the jet formed at the glottal opening. The upstream-propagating acoustic waves are generated by impingement of the coherent flow structures on the planar inner laryngeal wall, consisting of thyroid, and perhaps partially epiglottis. The resonance frequencies, f_n , require an integer number (n) of waves be present: $n = f_n (x/c + x/u)$, where x is the
65 distance between jet exit (glottis) and planar wall, i.e. impingement length (**Fig 1E**), u is the mean convection speed of the coherent structures, approximated as jet exit speed, and c is sound speed [7]. Because $u/c \ll 1$, the whistling frequency is given by: $f_n = n * u/x$. This model predicts multiple discrete whistling frequencies and can explain the different density gas observations in [3] (see Experimental Procedures). Furthermore, this model produces stable whistle frequencies only within a

70 narrow range of flow conditions, approximately when $d/x \leq St < 1$, where St is the Strouhal number
 $St = f_n * d/u$, with d the effective jet diameter.

To test this model we systematically changed jet speed u by altering subglottal pressure and
impingement length x with a metal plate after thyroid removal in four larynges. We could induce
whistles that exhibited stable whistling modes, jumps between modes, and concurrent modes in all four
75 larynges. The modal frequencies were accurately predicted by our model (**Fig 1F**), providing strong
support for our hypothesis that USVs are produced by a jet impinging on a planar wall.

What exact mechanism constitutes the feedback remains unknown; it could be either upstream
propagating acoustic disturbances through the core of the jet, or outside of the jet, or some edge effect
[7,8]. Furthermore, we currently cannot accurately predict which modes are stable and what triggers
80 jumps; the exact St values where modes are stable depends on the shear boundary layer properties at the
jet exit [8, 9]. We speculate jumps occur with sudden changes in jet speed as potentially found during
higher states of attention/arousal [10].

Our model predicts that stable modes are set by jet speed, effective diameter and distance from
glottis to thyroid, parameters controlled by combinations of intrinsic laryngeal anatomy, and respiratory
85 and laryngeal motor programs [6]. Our data therefore imply that the categorization of USV syllables
requires careful consideration, since current classifications in mice may represent random jumps
between stable modes that do not necessary reflect specific motor commands. Furthermore, our results
suggest that strain specific USVs or USV changes in mouse models of genetically linked human
communication disorders, such as autism, stuttering, and dyspraxia, may be the result of altered
90 laryngeal geometry as well as motor programs.

Supplemental Information

Supplemental Information including experimental procedures and two figures can be found with this article online at: ...

95

Acknowledgements

This work was supported by grants of the NSF (IOS 1257768) to CVP, Danish Research Council to CPHE. All experiments were conducted at the University of Southern Denmark in accordance with the animal care and use committee of the University of Southern Denmark. Furthermore, we like to thank Peter Bollen, Biomedical Laboratories, University of Southern Denmark, for obtaining the specimens.

100

References

1. Scattoni, M. L., Crawley, J., and Ricceri, L. (2009). Ultrasonic vocalizations: a tool for behavioural phenotyping of mouse models of neurodevelopmental disorders. *Neurosci. Biobehav. Rev.* 33 (4), 508-515.
2. Brudzynski, S. M. (2009). *Handbook of mammalian vocalization: an integrative neuroscience approach*, First Edition (London: Academic Press).
3. Roberts, L. H. (1975). The rodent ultrasound production mechanism. *Ultrasonics*. 13(2), 83-88.
4. Portfors, C. V., and Perkel, D. J. (2014). The role of ultrasonic vocalizations in mouse communication. *Curr. Opin. Neurobiol.* 28, 115-120.
5. Henrywood, R. H., and Agarwal, A. (2013). The aeroacoustics of a steam kettle. *Phys. Fluids*. 25(10), 107101.
6. Riede, T. (2013). Stereotypic laryngeal and respiratory motor patterns generate different call types in rat ultrasound vocalization. *J. Exp. Zool. A. Ecol. Genet. Physiol.* 319 (4), 213-224.

105

110

- 115 7. Ho, C. M., and Nosseir, N. S. (1981). Dynamics of an impinging jet. Part 1. The feedback phenomenon. *J. Fluid Mech.* 105, 119-142.
8. Rockwell, D., and Naudascher, E. (1979). Self-Sustained Oscillations of Impinging Free Shear Layers. *Annu. Rev. Fluid Mech.* 11, 67–94.
9. Morris, P. J. (1976). The spatial viscous instability of axisymmetric jets. *J. Fluid Mech.* 77 (3), 511.
- 120 10. Wang, H., Liang, S., Burgdorf, J., Wess, J., and Yeomans, J. (2008). Ultrasonic vocalizations induced by sex and amphetamine in M2, M4, M5 muscarinic and D2 dopamine receptor knockout mice. *PloS One.* 3(4), e1893.

125 **Figure 1. Mouse USVs are produced within the larynx by a planar impinging air jet.** A) Sagittally sectioned isolated mouse larynx. Bar = 1 mm. B) Extracted glottal dimensions from video still. The glottis consisted of the cartilaginous glottis between the arytenoids only. C) Elicited USVs in excised mouse larynges (N=5, color coded) show a clear increase of peak frequency with subglottal flow (top). The extracted glottal width (bottom) does not contain the frequency components the sound does and
130 therefore does not vibrate at those frequencies during USV production. D) Epiglottis and thyroid removal reduced USV production to 77% and 0% respectively in 7 larynges. USVs were rescued 100% by a metal plate replacement of the thyroid (N=5). E) Planar impinging jet model of mouse USV production with jet exit speed u and impingement length x . The feedback (red) travels back in the jet to the glottis. F) The planar impinging jet model accurately predicts observed frequency modes during
135 constant (left) and modulated impingement length x (right). Glottal area = 0.375 mm^2 . Unstable modes ($d/x \leq St < 1$) are depicted in orange. (FFT length: 1024, overlap: 75%, Hamming window, dynamic range: 50 dB).

140 **Experimental procedures**

Subjects

Because *in vivo* recordings have shown that female mice emit ultrasonic vocalizations with similar acoustic features as male mice [1], we used both males and females in our experiments. For *in vitro* experiments, 15 out of 17 larynges tested made ultrasonic sound. Of these 17 larynges tested, 10 were
145 adult BALB (male n = 4, female n = 6), 5 were adult C57 (male n = 4, female n = 1), and 2 were adult NMRI (female n = 2) mice from Taconic Europe, Denmark. Detailed video and acoustic analysis was conducted on 8 adult BALB (male n = 4, female n = 4) and 1 adult NMRI (male n = 1) mice. Of these larynges, *in vivo* recordings were recorded from 2 BALB males. All experiments were conducted at the University of Southern Denmark in accordance with the Danish Animal Experiments Inspectorate
150 (Copenhagen, Denmark).

Excised larynx preparation

Mice were euthanized with isoflurane and the larynx, trachea, lower jaw and tongue were dissected, flash frozen in liquid nitrogen, and then maintained at -80 C until just prior to the experiment. At the
155 start of each experiment, tissue was thawed in refrigerated ringer's solution [2] and the lower jaw, tongue, esophagus, hyoid, fat, and oropharynx were removed. The exterior, ventral, and dorsal views of each larynx were photographed with a Leica DC425 mounted on a stereomicroscope (M165-FC, Leica Microsystems). The trachea and attached larynx were fixed on a blunted 19G needle using 10-0 monofilament suture. Care was taken that the end of the needle was greater than 0.5 mm from the caudal
160 end of cricothyroid muscles. The arytenoids were held in place by two micromanipulators, but also without these USVs were readily elicited and all recordings were done with the larynx in resting

position, i.e. without additional adduction of the arytenoids. Tissue was kept moist during the experiment with Ringer's solution.

165 Once secured onto the needle, the trachea and larynx were set upright onto a custom made apparatus with computer controlled air delivery system. Air driven through the larynx was pressure controlled, humidified, and temperature monitored (temperatures ranged from 22 – 30°C) as described in detail in [3]. We subjected the larynx to an increasing and decreasing pressure ramp from 0-2 kPa in 4 s. Tracheal mass flow was measured with MEMS flow sensors (PMF series, Posifa Microsystems, San Jose, USA) and a response time of 1 ms. To our knowledge no calibrated subglottal pressure or tracheal
170 mass flow measurements during *in vivo* USV production are available for mice, but we consider the applied 0-2 kPa range physiologically relevant, because (1) in rats subglottal pressure ranges from 0-2 kPa during *in vivo* USV production [4,5], (2) in similarly sized birds subsyringeal pressures during song and induced sound production range from 0-3 kPa [3,6-8], and (3) increasing subglottal pressure above 3 kPa *in vitro* lead to a substantial increase of acoustic noise suggesting that the upper limit for stable
175 mode production was reached. The applied subglottal pressure ramps resulted in tracheal mass flow of 0-4 ml/s (Fig 1C). During quiet respiration in rats, tracheal mass flow is 15-20 ml/s/kg [9]. Extrapolating these values to a mouse of 20 gr would suggest a tracheal mass flow during quiet respiration of 0.3-0.4 ml/s, which is below, and thus consistent with, the observed phonation threshold flow of 1 ml/s in Fig 1C.

180 Sound was recorded with a 1/4 inch pressure microphone-pre-amplifier assembly (model 46BD, G.R.A.S., Denmark), amplified and high-pass filtered (10 Hz, 3-pole Butterworth filter, model 12AQ, G.R.A.S., Denmark). The microphone sensitivity was measured before each experiment (sound calibrator model 42AB, G.R.A.S., Denmark). The microphone was placed at 22-24 mm away from the mounted larynx in the acoustic near field, and on a 90° angle to avoid the air jet from the tracheal outlet.

185 Microphone, pressure and flow signals were low-pass filtered at 100, 10 and 10 kHz, respectively
(custom-built filter) and digitized at 250 kHz (USB 6259, 16 bit, National Instruments, Austin, Texas).
All control and analysis software was written in Matlab.

The laryngeal glottal opening was imaged with a light-sensitive 16 bit high-speed camera
(Fastcam SA1, Photron, San Diego, CA, USA; 100,000 frames/s) mounted on a stereomicroscope
190 (M165-FC, Leica Microsystems) and illuminated by a plasma light source (HPLS200, Thorlabs,
Germany) through liquid light guides. The glottis consisted of the cartilaginous glottis between the
arytenoids, and never reached into the membranous vocal fold portion. Due to the large amounts of data
collected when imaging at 100,000 fr/sec we typically recorded 1-2 seconds.

We developed an algorithm for automated parameter extraction of projected glottal area and
195 width per frame. After finding the glottal shape in each frame by Canny edge detection, the midline of
the glottis was defined as the major axes orientation of a fitted ellipsoid to the extracted shape. Glottal
width (i.e. arytenoid abduction times two) was calculated as the maximum of the perpendicular distance
between the midline and all points along the glottal shape. Due to the downward $\sim 45^\circ$ angle of the
glottis with the stereomicroscope's objective (see Fig 1A), the actual glottal area was about
200 $[1/\cos(45^\circ)=]$ 1.4 larger than the projected glottal area, and ranged from 0.1 to 0.45 mm² between
preparations, resulting in jet speeds around 10-15 m/s. Glottal width was parallel to the objective and
thus was correctly projected, and varied little within - but more between - preparations ranging from 36
to 80 pixels (0.33 to 0.73 mm). With Canny edge detection we could in principle not detect vibration
below a single pixel of 9.2 μm . To determine if we could detect smaller vibrations masked by noise, we
205 also inspected high dynamic range spectrograms of the glottal width signal. Careful visual inspection of
our raw image data, played-back at various relevant speeds, and the spectrograms of glottal width did
not reveal any motion at the frequencies of the USVs. Peak frequency in the glottal width signal was

finally determined by calculating power spectral density estimates of the glottal width of 500 consecutive images using the periodogram method (zero padded to 512 points). The peak frequency
210 always occurred at 0 Hz (Fig 1C).

We removed the epiglottis with a horizontal cut using micro-scissors. We subsequently cut slices of the cranial part of the thyroid until just above the vocal folds.

Wall impinging jet model

215 We derived our model from [10]. Resonance occurs when the feedback is in phase with the instability waves in the jet. The phase of the feedback disturbance at frequency f is given by $2\pi \cdot \left(f \frac{x}{u} + f \frac{x}{c}\right)$, where x is the distance between the jet exit (glottis) and the planar wall, i.e. the impingement length, u is the mean convection speed of the coherent structures, approximated as jet exit speed, and c is sound speed. This feedback phase will be in phase with the initial disturbance if equal to $2\pi \cdot n$, where n is an
220 integer, and thus follows: $n = f_n \left(\frac{x}{c} + \frac{x}{u}\right)$. Because $u/c \ll 1$, the whistling frequency is given by: $f_n = n * u/x$.

Jumps between modes thus need not be harmonically related. If the $n=1$ mode is observed the steps would be harmonics. In Figure 1F for example, $n=1$ is not excited, and thus the whistling frequencies are not harmonically related.

225 Our model predicts that the resonance frequencies are independent of the speed of sound if the jet speed remains constant. However, generating a whistle with the same pressure difference (from sub- to supraglottal) in a gas with lower density ρ results in a higher jet speed u that is inversely proportional to the square root of air density ($u \propto 1/\sqrt{\rho}$). Thus, from our model ($f_n = n * u/x$) follows that the predicted frequency of the whistle is inversely proportional to the square root of density ($f_n \propto 1/\sqrt{\rho}$).
230 However, a lower density gas also has a different speed of sound, which is *also* inversely proportional to

the square root of density, because $c = \sqrt{K/\rho} \propto 1/\sqrt{\rho}$, where K is an adiabatic constant. Thus, because both parameters are proportional to $1/\sqrt{\rho}$, jet speed u and the speed of sound c are directly proportional to each other, i.e. $f_n \propto c$. This relation explains Roberts' observations that rodent USV frequencies shifted upwards in heliox gas with an increased speed of sound compared to normal air [11].

235 Varying jet speed u between 0-20 m/s at a fixed impingent length x of 2 mm results already in a wide range of predicted frequencies up to 80 kHz for modes 1-8 (Figure S2A), and up to 160 kHz for $x=1$ mm. Recently it was shown that the USVs produced *in vivo* can have a wider range (20-100 kHz) [12] than the previously accepted range of 30-100 kHz [13] and our model thus covers the frequency range found both in our *in vitro* as well as *in vivo* observations.

240

Modulating impingement length

Mice probably only have a limited range to modulate the distance between glottis and thyroid wall, i.e. impingement length x . Most of the frequency modulation will therefore likely be driven by changes in jet speed u , by changing mass flow and glottis shape. Therefore we reasoned that changing laryngeal impingement length experimentally would provide further support for our model.

245 To modulate jet impingement length after thyroid removal, a 4x2 mm metal plate made out of a flattened 19G needle was placed at the original position of the thyroid (Figure S2B). The precise position and motion of this plate was controlled with an ergometer (Model 300C, Aurora Scientific, Ontario, Canada), which measured displacement at the tip of the lever arm (displacement resolution 1 μm). The larynges were placed in the setup as described above with a constant jet speed (10-30 ml/s) in combination with no movement, or sinusoidal movement of the plate.

250

To determine the impingement length x , we quantified the exact position of the plate and glottal opening by filming the larynx with a high-speed camera (MotionPro-X4, 12 bit CMOS sensor, IDT; 500 frames/s) simultaneously from the top and side by placing a 5x5x5 mm 45° angled aluminium surface-coated prism (Thorlabs, Newton, New Jersey, US) next to the larynx. Because the plate often obscured the glottal opening only the side views were used for extraction of plate position and impingement length. To calculate the exact position of the plate (wall) and glottal opening (jet exit) we cross-correlated regions of interest containing only the plate or larynx with the entire image. We used linear interpolation to position the peak in the cross-correlation at a precision of 2.54 μm .

The mean convection speed of the coherent structures is approximated as jet exit speed u , which we calculated as the measured tracheal mass flow divided by glottal area. Because we could not directly measure glottal area in this experiment, we needed to fit the area to obtain the measured sound frequency traces. In all four larynges the area was 0.2 – 0.4 mm^2 , values that corresponded well with values observed in the intact excised larynx experiments (0.1 – 0.45 mm^2).

In vivo vocalization recordings

USVs emitted in the presence of a familiar female mouse were recorded from two adult (>100 days) male mice prior to *in vitro* experiments. The females were devocalized by unilateral nerve cut [14]. Mice were placed into a standard acrylic cage located within a single walled attenuating chamber. USVs were recorded with a ½ inch G.R.A.S. (type 26AC) high frequency microphone placed 10 cm above the cage floor. The acoustic signals were amplified and digitized by an Avisoft Bioacoustics amplifier at a sampling rate of 250 kHz and 16-bit resolution.

275 **USV Analysis**

Acoustic parameters of all in vitro and in vivo USVs were analyzed using Avisoft SASLab Pro software (Avisoft Bioacoustics), as described in detail in [15]. USVs were automatically detected by the software when energy was above a certain threshold, bounded by $> - 2$ ms of silence, minimum duration of 1 ms, and hold time of 20 ms. For each USV, the minimum, maximum, and mean peak frequencies were
280 extracted from spectrograms of each USV (Hamming window, 1024 FFT length, 100% frame size, 85% temporal overlap). Because maximum peak frequencies were measured from the highest frequency bin of the detected signal, USVs with multiple modes had higher max frequencies than those with only one mode.

285 **Methods References**

- [1] Hammerschmidt K., Radyushkin K., Ehrenreich H., Fischer J. (2012). The structure and usage of female and male mouse ultrasonic vocalizations reveal only minor differences. *PLoS One*. 7(7): e41133.
- [2] Elemans, C. P. H., Spierts, I. L. Y., Hendriks, M., Schipper, H., Müller, U. K., and Van Leeuwen, J. L. (2006). Syringeal muscles fit the trill in ring doves (*Streptopelia risoria* L.). *J. Exp. Biol.* 209 (5), 965-
290 977.
- [3] Elemans C.P.H. *et al.* (2015) Universal mechanisms of sound production and control in birds and mammals. *Nat. Commun.* 6:8978
- [4] Riede, T. (2011). Subglottal pressure, tracheal airflow, and intrinsic laryngeal muscle activity during rat ultrasound vocalization. *J. Neurophysiol.* 106 (5), 2580–2592.
- 295 [5] Riede, T. (2013). Stereotypic laryngeal and respiratory motor patterns generate different call types in rat ultrasound vocalization. *J. Exp. Zool. A. Ecol. Genet. Physiol.* 319 (4), 213-224.

- [6] Elemans C.P.H., Zaccarelli R., Herzel H. (2008). The biomechanics and neuromuscular control of vocalisation in a non-songbird. *J. R. Soc. Interface.* 5, 691-703.
- [7] Elemans CPH, Laje R, Mindlin GB, Goller F (2010). Smooth operator: Avoidance of subharmonic bifurcations through mechanical mechanisms simplifies song motor control in adult zebra finches. *J. Neurosci.* 30, 13246–13253.
- [8] Riede, T. and Goller, F. (2010). Peripheral mechanisms for vocal production in birds – differences and similarities to human speech and singing. *Brain. Lang.* 115, 69–80.
- [9] Mortola, J. P., and Noworaj, A. (1983). Two-sidearm tracheal cannula for respiratory airflow measurements in small animals. *J. Appl. Physiol. Respir. Environ. Exerc. Physiol.* 55(1 Pt 1), 250–253.
- [10] Ho, C. M., and Nosseir, N. S. (1981). Dynamics of an impinging jet. Part 1. The feedback phenomenon. *J. Fluid Mech.* 105, 119-142.
- [11] Roberts, L. H. (1975). The rodent ultrasound production mechanism. *Ultrasonics.* 13(2), 83-88.
- [12] Grimsley, J. M., Sheth, S., Vallabh, N., Grimsley, C. A., Bhattal, J., Latsko, M., and Wenstrup, J. J. (2016). Contextual Modulation of Vocal Behavior in Mouse: Newly Identified 12 kHz “Mid-Frequency” Vocalization Emitted during Restraint. *Front. Behav. Neurosci.* 10.
- [13] Sales, G. D. (1972). Ultrasound and mating behaviour in rodents with some observations on other behavioural situations. *J Zool*, 168, 149-164.
- [14] Nunez, A. A., Pomerantz, S. M., Bean, N. J., and Youngstrom, T. G. (1985). Effects of laryngeal denervation on ultrasound production and male sexual behavior in rodents. *Physiol. Behav.* 34 (6), 901-905

- [15] Mahrt, E. J., Perkel, D. J., Tong, L., Rubel, E. W., and Portfors, C. V. (2013). Engineered deafness reveals that mouse courtship vocalizations do not require auditory experience. *J. Neurosci.* 33 (13), 5573-5583.

320

325

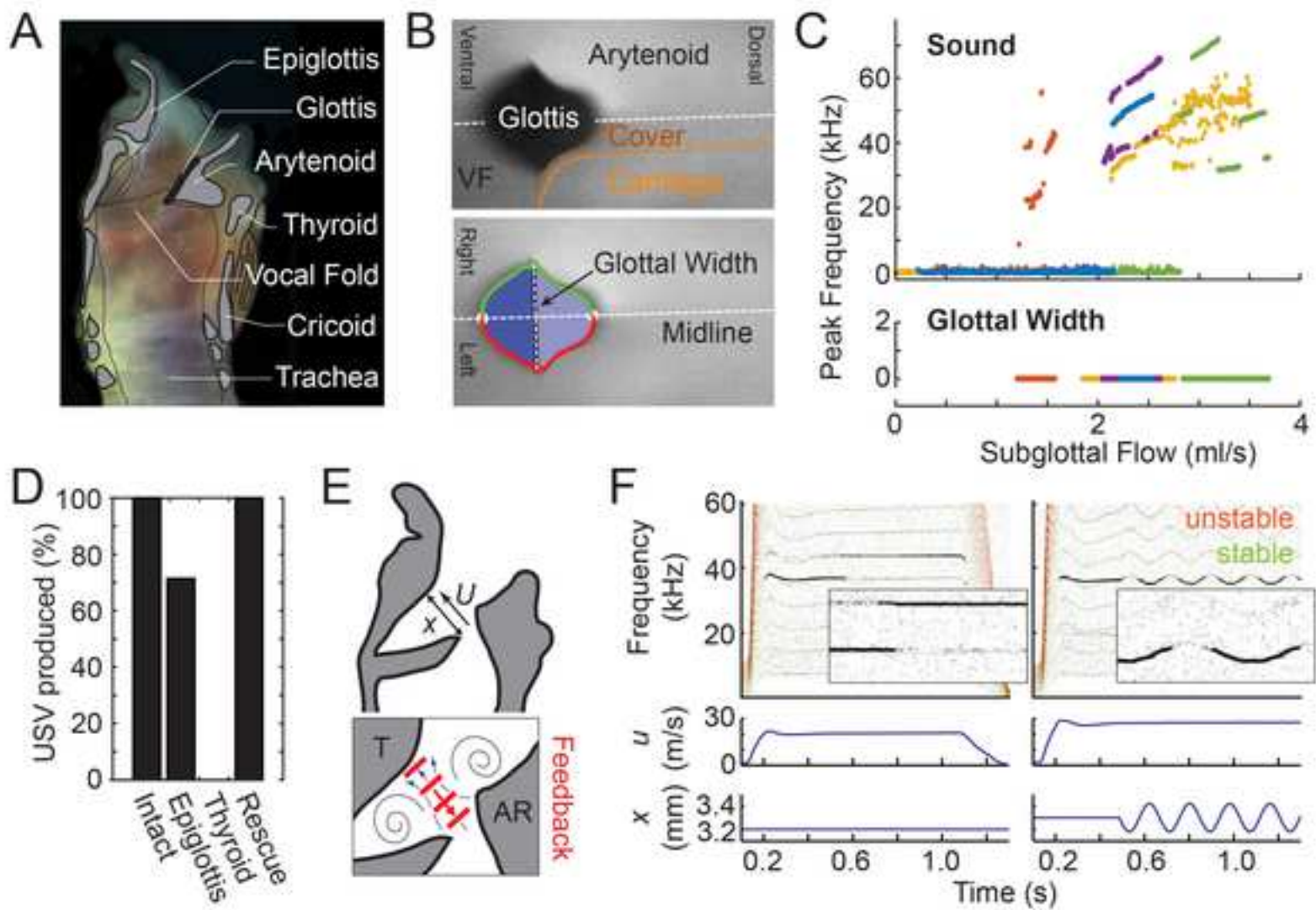


Figure S1

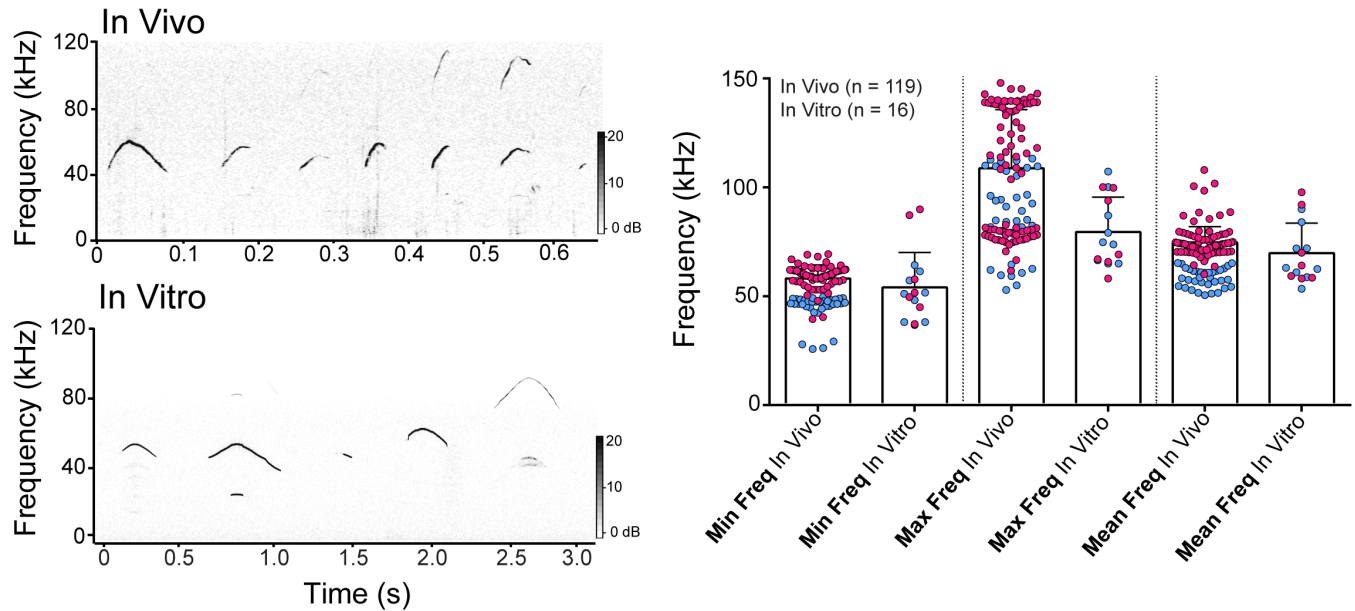
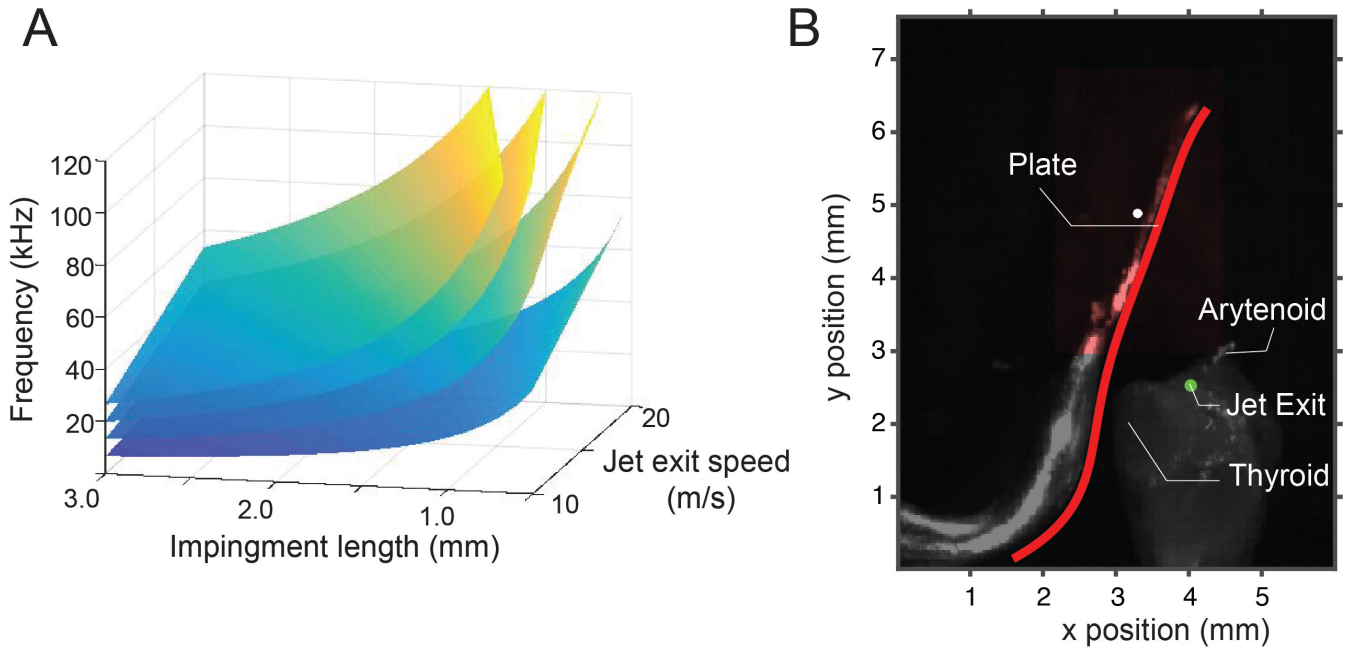


Figure S1. USVs and UVs produced by the excised larynx *in vitro* correspond well to *in vivo* USVs.

- A) Exemplary spectrograms of in vivo (top) and in vitro USVs (bottom) (FFT length: 1024, overlap: 75%, Hamming window; dynamic range: 20 dB) B) Minimum and mean peak frequency of USV and f-
- 5 USV were not significantly different (Student's T-Test; $P > 0.01$), while max frequency was greater in the *in vivo* prep (Student's T-Test; $P < 0.01$). Blue colored circles represent sound repetitions from one animal and pink from another animal from in vivo and in vitro conditions.



10

Figure S2. Testing frequency mode predictions of the planar wall impinging jet model. A) Surface plot of predicted whistle frequencies as function of jet flow and impingement length. Only modes $n=2$, 4, 6, and 8 are shown for clarity. B) Sideview (movie still) of thyroid replacement experiment showing the extracted boundary of plate (red line) that was positioned by cross-correlating the plate (red shading) with the image. The white dot indicates the subpixel position of the center of the plate sub-image used for cross-correlation. The green dot is the estimated exit position of the glottal jet. The upper part of the thyroid is cut away. Pixel resolution in the original image was $25.4 \mu\text{m}$.

15

20